Polyhedron 30 (2011) 1538–1546

Contents lists available at ScienceDirect

Polyhedron

journal homepage: www.elsevier.com/locate/poly

Photophysical properties and photocytotoxicity of novel phthalocyanines – potentially useful for their application in photodynamic therapy

Tomasz Goslinski [a], Tomasz Osmalek [b], Krystyna Konopka [c], Marcin Wierzchowski [a], Piotr Fita [d,e], Jadwiga Mielcarek [b,*]

[a] Department of Chemical Technology of Drugs, Poznan University of Medical Sciences, Grunwaldzka 6, 60-780 Poznan, Poland
[b] Department of Inorganic and Analytical Chemistry, Poznan University of Medical Sciences, Grunwaldzka 6, 60-780 Poznan, Poland
[c] Department of Biomedical Sciences, University of the Pacific, Arthur A. Dugoni School of Dentistry, San Francisco, USA
[d] Department of Physical Chemistry, University of Geneva, 30 quai Ernest-Ansermet, CH-1211 Geneva 4, Switzerland
[e] Institute of Experimental Physics, Faculty of Physics, University of Warsaw, Hoza 69, 00-681 Warsaw, Poland

ARTICLE INFO

Article history:
Received 18 January 2011
Accepted 3 March 2011
Available online 17 March 2011

Keywords:
Photocytotoxicity
Photosensitizer
Phthalocyanine
Singlet oxygen
Solvatochromic effect
PDT

ABSTRACT

Two novel zinc(II) phthalocyanines bearing non-peripheral ester-alkyloxy substituents (**Pc-4** and **Pc-5**) were synthesized, by a two-step procedure starting from 2,3-dicyanohydroquinone. Both sensitizers show promising photophysical properties, including solvatochromic study, qualitative evaluation of emission, aggregation behavior and singlet oxygen generation. It was proven that the photodynamic activity of the compounds studied depends on the molecular oxygen level. Comparison of the quantum yields of singlet oxygen generation as well as the oxidation rate constants using 1,3-diphenylisobenzofurane before and after deaeration proved the photodynamic effect of **Pc-4** and **Pc-5** to be governed by the photosensitization mechanism II. Changes in the quantities of the compounds exposed to irradiation were also estimated. Upon their exposure to light the changes in intensity of the Q band were monitored. The photodecomposition of **Pc-4** and **Pc-5** in DMSO or DMF solutions was found to proceed according to the first order kinetic reaction in two stages.

The photosensitizing effect of **Pc-4** in HSC-3 cells was significantly lower than that of **ZnPc**. **Pc-4** was ineffective at 0.1 μM, while a low, approx. 15% photocytotoxicity was observed at 5 μM, at a distance of 5 and 10 cm. The efficacy of **Pc-4** in photokilling of cultured cells is affected by hydrophobicity and the aggregation status of the photosensitizer.

1. Introduction

There is a large variety of macrocyclic compounds in our environment. They play an essential role in regulation of many biological processes such as cell growth or electron transfer during photorespiration. Metallophthalocyanines can be considered as synthetic porphyrin analogs. They possess a conjugated system of π-electrons and exhibit the ability to chelate metal ions in the center of the ring [1–3].

The first phthalocyanine was synthesized in 1907 and for next 20 years copper and iron complexes were used mainly as green and blue dyestuffs in polygraphic and textile industry. A remarkable increase of interest in potential applications of metallophthalocyanines began in 1930. In addition to classical substitution reactions, phthalocyanine ring can be modified by a variety of different functional groups [4,5]. Unique physicochemical properties of new derivatives found applications in production of liquid crystals, Langmuir–Blodgett films, gas sensors, optoelectronic devices or catalytic materials. Phthalocyanines are also considered to be one of the most promising compounds in the field of nanotechnology [6–12]. It turned out that photoinduced electron transfer properties of covalently linked phthalocyanine–fullerene dyads are much more advantageous than classical porphyrin systems [13].

The photosensitizing activity provides the opportunity to employ phthalocyanines as active agents for photodynamic therapy in medicine [14–17]. Efficient singlet oxygen generation, high stability toward temperature and irradiation, desirable spectroscopic features and low dark toxicity contribute to the fact that phthalocyanines are currently one of the most potent and promising photosensitizers.

A very low solubility of phthalocyanines in common organic solvents has been the main hindrance for their desired activities [18,19]. Unsubstituted or metal-free analogs are almost insoluble and new synthetic methods should be designed for derivatives containing appropriate functional groups such as amide, carboxylic or sulfonic [20–22]. The introduction of long-chain substituents to the periphery is expected to prevent the aggregation [23]. On the

* Corresponding author. Tel.: +48 61 854 66 04; fax: +48 61 854 66 09.
E-mail address: jmielcar@ump.edu.pl (J. Mielcarek).

0277-5387/$ - see front matter © 2011 Elsevier Ltd. All rights reserved.
doi:10.1016/j.poly.2011.03.003

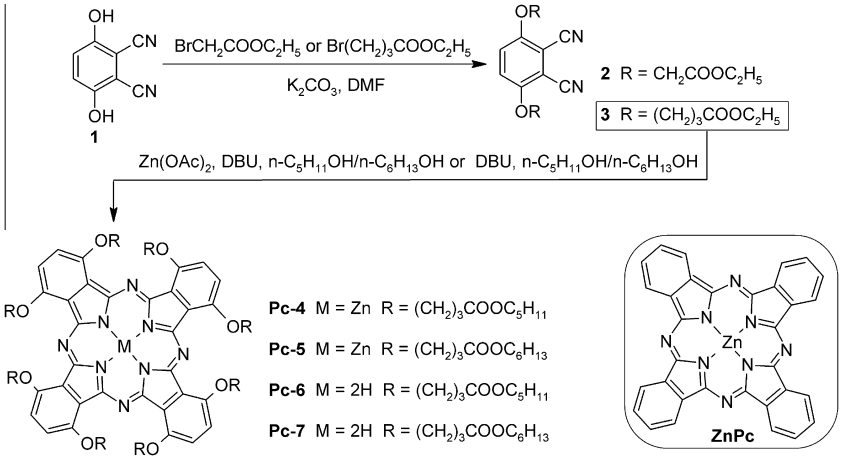

Scheme 1. Preparation of phthalonitriles **2**, **3**, and phthalocyanines **Pc-4–Pc-7.**

other hand, the low solubility of most phthalocyanines in water can be bypassed by the use of liposomes, emulsions or nanoparticle carriers [24–26].

Because zinc phthalocyanines satisfy almost all requirements for a "good photosensitizer", they are currently the most widely tested dyes for Photodynamic Therapy (PDT) – (Scheme 1, inset). This work reports on the photophysicochemical and biological properties of novel phthalocyanines possessing non-peripheral ester-alkyloxy substituents.

2. Results and discussion

2.1. Synthesis

According to a modified literature procedure [27,28] phthalonitriles **2** and **3** were prepared by the alkylation of the inexpensive, commercially available 2,3-dicyanohydroquinone **1** with ethyl bromoacetate and ethyl 4-bromobutyrate in the presence of K_2CO_3 in dimethylformamide (DMF) at 70 °C for 24 h, respectively (Scheme 1). While the alkylation of **1** was performed with ethyl 3-bromopropionate, an elimination reaction within the alkylating agent occurred. The resulting hydroquinone dialkylated ether **2** decomposed under macrocyclic reactions conditions. The dinitrile **3** was found to be unreactive under the normal Linstead macrocyclization conditions (a suspension of magnesium butoxide in refluxing butanol) [29]. Therefore it was necessary to use harsh conditions by heating at 130 °C for 24–72 h in 1-pentanol or 1-hexanol in the presence of 1,8-diazabicyclo[5.4.0]undec-7-ene (DBU) as a base with or without metal salt [30]. Thus reaction performed with zinc acetate led to the desired zinc phthalocyanines **Pc-4**, **Pc-5**, whereas the reaction performed without metal salt source led to the demetallated phthalocyanines **Pc-6**, **Pc-7**. It is noteworthy that during macrocyclization reaction parallel transesterification reaction within the peripheral ester-alkyloxy chains occurred.

All macrocyclic products **Pc-4–Pc-7** were purified by column chromatography and isolated as dark green films in yields of 7.6%, 0.4%, 1.6% and 4.7%, respectively. HPLC analysis revealed the purity of samples **Pc-4** and **Pc-5** to be at the level 97.5–97.7% and 97.6%, respectively. Phthalocyanines **Pc-6** and **Pc-7** were found unstable under standard conditions (room temperature and access to day light) as the photobleaching took place very fast, which was monitored by HPLC. The ^{1}H NMR spectra of phthalocyanines **Pc-4–Pc-7** in pyridine-d_5 showed 1 singlet at δ 7.86–7.88 ppm for the phthalocyanine β-ring protons. The connectivities found in COSY (Correlation Spectroscopy), HMQC (Heteronuclear Multiple Quantum Correlation) and HMBC (Heteronuclear Multiple Bond Coherence) spectra of **Pc-4** and **Pc-7** enabled to attribute all protons and carbons within the structure of the ester-alkyloxy substituent and phthalocyanine core (Tables 1S and 2S, Supplementary material).

2.2. Photochemical and solvatochromic studies

The electronic absorption spectra of **Pc-4** and **Pc-5** revealed characteristic features of the phthalocyanine spectra. They show a low intensity Soret band (B band) in the range of 300–400 nm and a much more intense Q band in the range of 600–900 nm. The significant intensity of this band has been a result of the π–π* transitions in macrocyclic system. According to the literature, the Q band present in the UV–Vis spectra of phthalocyanines in comparison with other porphyrinoids has been found significantly red shifted and more intense in relation to that of the B band [19]. The positions and intensities of some bands, especially Q band, have been also affected by the type of solvent used [31]. As follows from Fig. 1, for the majority of solvents, the Q band was split into a few components of similar or of different intensities. The separation of the resulting sub-bands strongly depended on the properties of the solvent, which eliminated vibrational structure as the origin of this splitting.

In the UV–Vis spectra of **Pc-4** and **Pc-5** recorded in 2-propanol, triethylamine, dioxane, N,N-dimethylformamide (DMF), N,N-dimethylacetamide (DMA) and dimethylsulfoxide (DMSO), the intense Q band was slightly split into the main one and the blue shifted (λ_{max} = 655–665 nm) side Q bands (Table 1). At the same time, the molar absorption coefficient of the rising edge was over three times smaller than that of the main component of the Q band. Among all the solvents considered, only in methanol the Q band was split into three components of different intensities, possibly as a result of the axial coordination of the Zn(II) ion by methanol. The main Q band component was present at λ_{max} = 735 nm and the two small bands, one at each side of the Q band, at λ_{max} = 660 and 820 nm, respectively. The band at λ_{max} = 660 nm has been often referred to as the X band appearing as a result of deformation of the phthalocyanine ring in some solvents [33].

It was found that the Q band red shifts were the greatest when chloroform and acetonitrile were used as solvents. The complex Q band spectra of **Pc-4** and **Pc-5** in chloroform possess a broad rising shoulder on which two components could be discerned at 761 and 806 nm, accompanied by an additional poorly developed band in the range of 410–530 nm. These features could be explained by strong solvation effects of the solvents. The spectra of **Pc-4** and **Pc-5** recorded in ethyl ether, ethyl acetate, hexane and cyclohexane revealed broad complex Q bands in the range of 600–

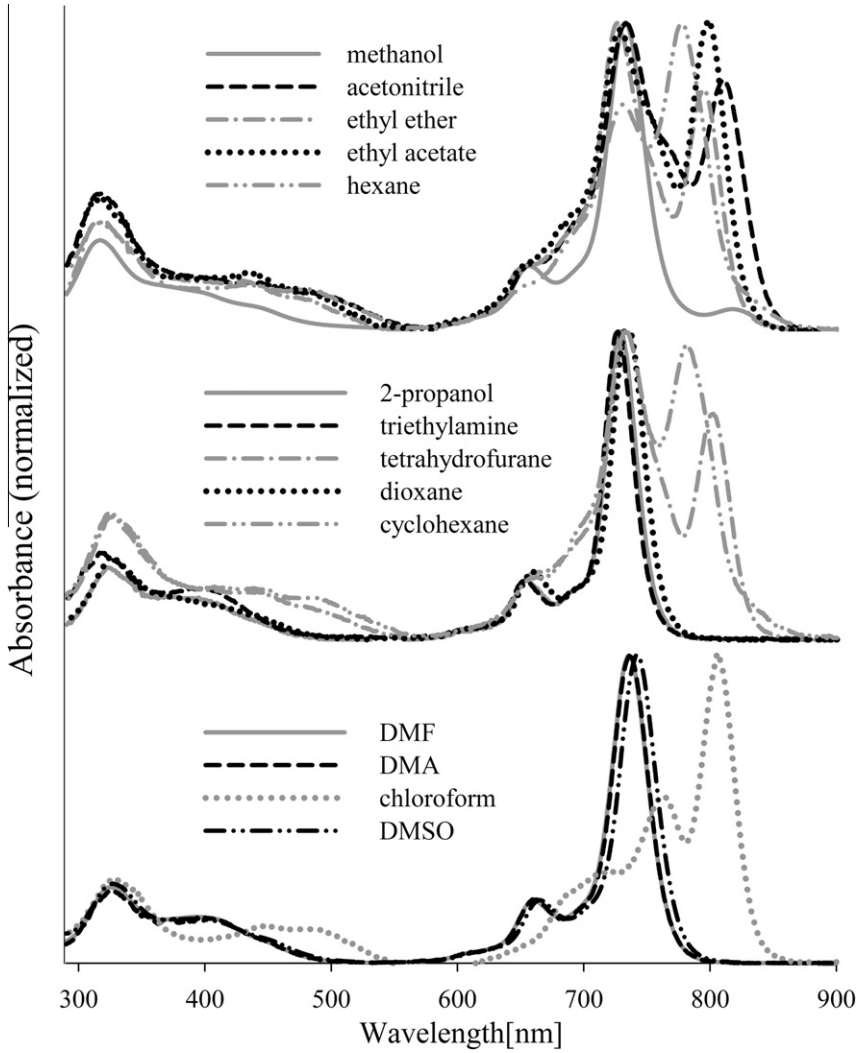

Fig. 1. Normalized UV–Vis spectra of **Pc-4** in various solvents.

Table 1
UV–Vis spectral data of **Pc-4** and **Pc-5** in various organic solvents (dipole moments and refractive indices [32]).

Solvent	Refractive index (20 °C)	Dipole moment (D)	**Pc-4**				**Pc-5**			
			B-band (nm)	Q-band (nm)			B-band (nm)	Q-band (nm)		
Methanol	1.328	1.70	326	660	735	820	326	660	735	820
Acetonitrile	1.344	3.92	327		736	811	328	736	767	811
Diethyl ether	1.352	1.15	328		730	796	326		730	797
Ethyl acetate	1.372	1.78	328		731	799	323		732	799
Hexane	1.375	0.00	327		733	779	329		732	780
2-Propanol	1.377	1.56	322	655	729		327	655	729	
Triethylamine	1.401	0.66	318	651	727		336	654	727	
THF	1.407	1.69	325		733	802	327		734	801
1,4-Dioxane	1.422	0.00	326	660	734		326	661	734	
Cyclohexane	1.426	0.00	323		733	782	326		733	781
DMF	1.430	3.82	326	660	736		327	661	733	
DMA	1.438	3.70	325	660	736		323	660	736	
Chloroform	1.446	1.04	326		761	806	330		762	806
DMSO	1.478	1.80	327	665	743		327	665	743	

870 nm, which were split into two components of similar intensities. As it could be seen in Table 1, small structural differences in the periphery did not influence significantly the spectra and solvatochromic effects. The Soret band and Q band ranges were similar, with minor differences in intensities and shifts.

The correlation between the Q band shift towards longer wavelengths and the refractive index of the solvent was tested to evaluate the solvatochromic effects [34]. The wavelength corresponding to the maximum of the Q band, λ_{max}, was plotted against the rational function $(n^2-1)/(2n^2+1)$ of the solvent's

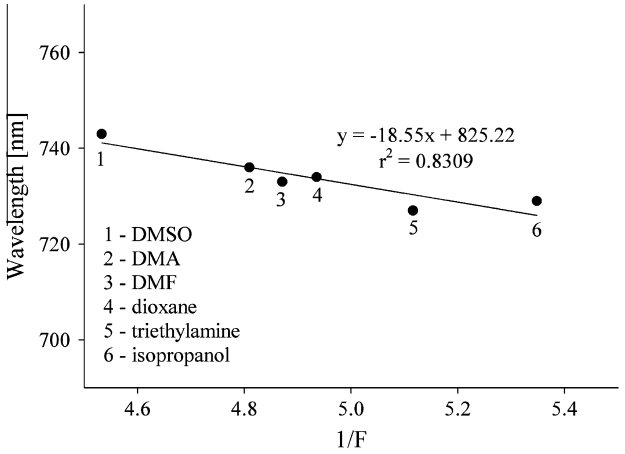

Fig. 2. Plot of wavelength λ_{max} of the Q band vs. the refractive index of the solvent described by the rational function $F = (n^2 - 1)/(2n^2 + 1)$; where n stands for the refractive index.

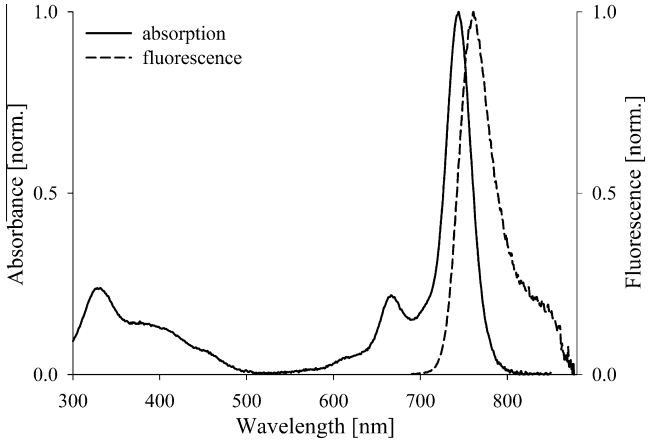

Fig. 4. Absorption and emission spectra of **Pc-4** in DMSO; excitation wavelength at 670 nm.

refractive index n (Fig. 2) according to the procedure [34]. This dependence is linear even though the influence of the solvent's dielectric constant on the solvatochromic shift is neglected here. Simultaneously, it was checked that for **Pc-4** and **Pc-5** the Q band shift was not correlated with the dipole moments of the solvents tested. Therefore it can be concluded that for 2-propanol, triethylamine, dioxane, DMF, DMA and DMSO the fast solvation due to solvent's polarizability (described by the refractive index) prevails over the slow solvation resulting from reorientation of the solvent's molecules (which would disturb the linear dependence shown in Fig. 2 and should be correlated with the dipole moment of the solvent's molecules).

The aggregation behavior of **Pc-4** and **Pc-5** were studied at different concentrations in DMSO and DMF (Fig. 3). The absorption of the Q band increased proportionally to the concentration of the compounds and no new bands that could be attributed to the aggregated forms were found [35]. The Beer–Lambert law was obeyed for each compound in all solvents.

2.3. Emission properties

Qualitative evaluation of emission, including quantitative analysis of the fluorescence spectra and determination of the quantum yields (Φ_f) was performed for **Pc-4** and **Pc-5**.

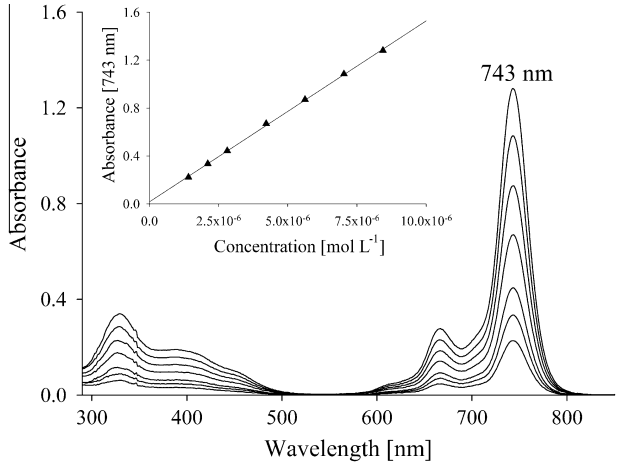

Fig. 3. Representative absorption spectra of **Pc-4** in DMSO; concentrations from 1.41 to 8.44 × 10^{-6} mol L^{-1}.

As it can be seen in Fig. 4 and Fig. 1S (Supplementary material), the emission spectra of **Pc-4** and **Pc-5** are consistent with both the Stokes rule and the rule of mirror symmetry between the absorption and fluorescence bands. The emission properties of **Pc-4** and **Pc-5** in DMSO were evaluated by comparison with those of **ZnPc** possessing no peripheral substituents. For **ZnPc** the Stokes shift was small ($\Delta\lambda$ = 7 nm) which confirms that the geometry of the molecule in the singlet excited state S_1 does not differ much from that in the ground state. The Stokes shift in the emission spectra of phthalocyanines possessing peripheral substituents was somewhat greater.

Fluorescence quantum yields (Φ_F) were determined by the comparative method according to the formula [36]

$$\Phi_{f,p} = \frac{\int F_p(\lambda)}{\int F_{qc}(\lambda)} \cdot \frac{1 - 10^{-Aqc}}{1 - 10^{-AP}} \cdot \Phi_{f,qc}$$

where $\Phi_{f,p}$ is fluorescence quantum yield of the sample; $\Phi_{f,qc}$ is fluorescence quantum yield of the standard; F_p is fluorescence intensity of the sample; F_{qc} is fluorescence intensity of the standard; A_p is absorbance of the sample at the excitation wavelength; and A_{qc} is the absorbance of the standard at the excitation wavelength.

The emission spectra of **Pc-4** and **Pc-5**, similarly to the absorption ones, depend on the presence of heteroatoms in the macrocyclic periphery (Table 2). Therefore a decrease of fluorescence quantum yield to the level of Φ_f = 0.06 in comparison to that observed for **ZnPc** (Φ_f = 0.2) was noticed [37]. This process has been related to the presence of free electron pairs at the oxygen atoms substituted to the non-peripheral positions of **Pc-4** and **Pc-5**, which facilitates the nonradiative quenching being the result of their coupling with the π-electron system of the phthalocyanine ring.

2.4. Singlet oxygen generation; Φ_Δ

Singlet oxygen quantum yields in DMSO were almost equal for **Pc-4** and **Pc-5** but lower than that of **ZnPc** [15]. This proves that

Table 2
Emission wavelengths, Stokes shifts values and fluorescence quantum yields at different excitation wavelengths for **Pc-4** and **Pc-5** in DMSO.

Compound	Emission λ_{max} (nm)	Stokes shift		Φ_f (excitation at Soret band)	Φ_f (excitation at Q band)
		$\Delta\lambda$ (nm)	(cm^{-1})		
ZnPc	678	7	150	0.20 ± 0.03 [37]	
Pc-4	761	18	350	0.066 ± 0.011	0.05 ± 0.02
Pc-5	761	18	350	0.067 ± 0.011	0.07 ± 0.02

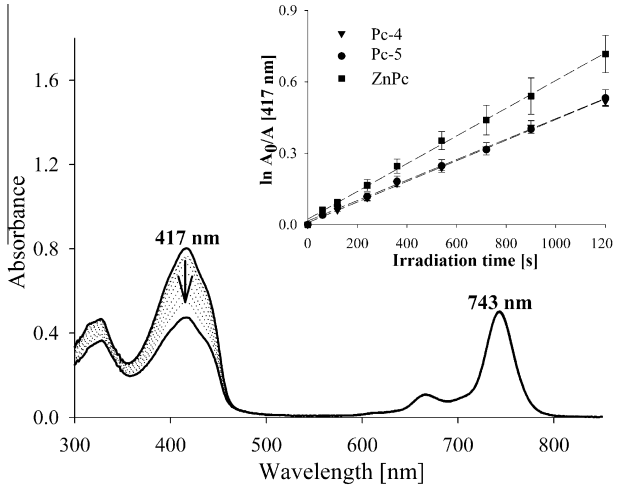

Fig. 5. Changes in the UV–Vis spectrum of DPBF and **Pc-4** in DMSO and first-order plots for oxidation of DPBF photosensitized by **Pc-4**, **Pc-5** and **ZnPc** in DMSO under aerobic conditions.

Table 3
Kinetic parameters describing relationships $\ln(A_0/A) = f(t)$ and quantum yields generation of singlet oxygen by phthalocyanine **Pc-4** and **Pc-5** in the presence of oxygen and after deaeration.

Solvent	Compound	Aerobic conditions	After deaeration	
		$10^4 \times (k \pm \Delta k)$ (s^{-1})	Φ_Δ	$10^4 \times (k \pm \Delta k)$ (s^{-1})
DMSO	**Pc-4**	4.34 ± 0.19	0.50	2.90 ± 0.30
	Pc-5	4.29 ± 0.21	0.49	2.59 ± 0.37
	ZnPc	5.83 ± 0.47	0.67 [38]	3.77 ± 0.14
DMF	**Pc-4**	7.10 ± 0.25	0.80	4.36 ± 0.59
	Pc-5	5.76 ± 0.34	0.65	4.84 ± 0.47
	ZnPc	4.99 ± 0.18	0.56 [38]	3.04 ± 0.21

non-peripheral substitution by eight long chain ester groups slightly reduces the ability to photosensitization. Distinct differences were found in DMF, where **Pc-4** exhibited stronger photosensitizing ability than **Pc-5** and **ZnPc** –Fig. 5.

It was also proven that the photodynamic activity of the compounds studied depends on the molecular oxygen level, as bubbling with nitrogen *via* reaction vessel for 20 min led to distinct inhibition of the 1,3-diphenylisobenzofurane (DPBF) oxidation – Table 3.

Comparison of the quantum yields of singlet oxygen generation as well as the oxidation rate constants using DPBF before and after deoxygenation has proved the photodynamic effect of **Pc-4** and **Pc-5** to be governed by the photosensitization mechanism II. After absorption of a photon by the photosensitizer and the subsequent intersystem crossing to the triplet state, the energy was transferred directly onto the oxygen molecule leading to formation of singlet oxygen with strong oxidizing properties.

2.5. Photostability assay

Energies and lifetimes of the excited states of the porphyrin molecules depend on the molecular structure of the complex with metal ions and the nature of the solvent. The greatest effect on stability of excited molecules exerts the stability of bonds in the macroring and the type of metal ion at the center of the molecule [39]. For **Pc-4** and **Pc-5** the redox processes involving Zn(II) ions should be excluded and the changes caused by this process should be related only to the macroring transformations. The excitation of the ring accompanied by oxidation process led to its decomposition into small fragments that do not absorb light in the UV–Vis. This

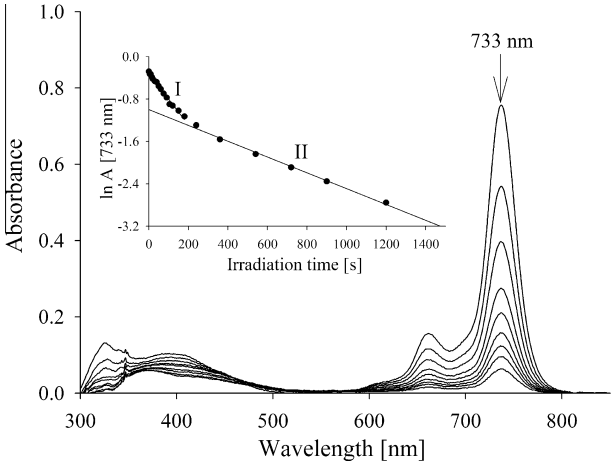

Fig. 6. Changes in the UV–Vis spectrum of **Pc-4** in DMSO during irradiation. The inset plot shows semilogarithmic dependence of $\ln A_{733\ nm}$ vs. time.

mode of decomposition of the phthalocyanine molecule, accompanied by systematic decoloration of the solutions, photobleaching, was reflected by the changes observed in the UV–Vis spectra. As shown in Fig. 6, on exposure of **Pc-4** and **Pc-5** solutions to irradiation the intensity of the Q band decreased and later this band disappeared.

Changes in the quantities of the compounds exposed to irradiation were also estimated. Upon their exposure to light the changes in intensity of the Q band were monitored. The photodecomposition of **Pc-4** and **Pc-5** in DMSO or DMF solutions was found to proceed according to the first order kinetic reaction in two stages.

The rate constants of the reaction (k_{1obs} and k_{2obs}) were found from the equation

$$\ln(A_t - A_\infty) = \ln(A_0 - A_\infty) - k_{obs} \cdot t$$

where A is absorbance in $t_0 \rightarrow t_\infty$; k_{obs} is the reaction rate constant [s^{-1}], and t is the time [s].

The rate constant of the second stage of the reaction (k_{2obs}) was found by subtraction. Comparison of k_{1obs} and k_{2obs} presented in Table 4 indicates that the first stage of the reaction is about 10 times faster than the second one.

2.6. Biological activity

HSC cells were incubated with **ZnPc** or **Pc-4** for 24 h in serum free medium. Cell viability was quantified by the Alamar Blue assay and expressed as the percentage of control cells (DME/0.5% DMSO). Data represent the mean ± SD from two independent experiments performed in triplicate.

HSC-cells were incubated with **ZnPc** or **Pc-4** for 24 h and exposed to light as described in Section 4. Cell viability was quantified by the Alamar Blue assay and expressed as the percentage of control cells not exposed to light. Data represent the mean ± SD from two independent experiments performed in triplicate.

Table 4
Rate constants values for particular stages of **Pc-4** and **Pc-5** photodecomposition in DMF.

Compound	$10^2 \times (k_{obs} \pm \Delta k_{obs})$ (s^{-1})	$10^3 \times (k_{obs} \pm \Delta k_{obs})$ (s^{-1})
Pc-4	I	II
	1.22 ± 0.10	1.49 ± 0.01
Pc-5	I	II
	1.20 ± 0.09	1.43 ± 0.09

Table 5
Dark toxicity of **ZnPc** and **Pc-4** in HSC-3 cells.

Compound	Cell viability (%)	Compound	Cell viability (%)
Control	100.0 ± 3.6	Control	100.0 ± 3.8
ZnPc 0.1 μM	103.3 ± 2.8	**Pc-4** 0.1 μM	110.8 ± 1.5
ZnPc 5 μM	96.9 ± 2.8	**Pc-4** 5.0 μM	101.1 ± 4.9

Table 6
Light-dependent toxicity of **ZnPc** and **Pc-4** in HSC-3 cells.

Distance (cm)	5		10	
Time (min)	0	20	0	20
Control	100.0 ± 8.7	100.0 ± 10.0	100.0 ± 5.6	100.0 ± 2.3
ZnPc 0.1 μM	111.8 ± 8.7	70.5 ± 6.2[y]	99.1 ± 12.0	103.5 ± 11.9
ZnPc 5 μM	113.1 ± 7.9	0	101.5 ± 7.1	0
Control	100.0 ± 2.3	100.0 ± 6.5	100.0 ± 1.2	100.0 ± 8.0
Pc-4 0.1 μM	99.2 ± 6.5	92.2 ± 1.8	102.3 ± 0.3	90.8 ± 7.7
Pc-4 5 μM	92.8 ± 6.5	87.8 ± 1.8[a]	91.2 ± 6.8	86.5 ± 6.1[x]

[a]Significantly different compared with contral : a– ($P < 0.025$); x – ($P < 0.05$); y – ($P < 0.005$).

The dark-toxicities of **ZnPc** and **Pc-4** in HSC-3 cells are presented in Table 5. At concentrations of 0.1 and 5.0 μM, **ZnPc** and **Pc-4** did not aggregate, and did not reduce the viability of HSC-3 cells. Significant, dose-dependent aggregation of **Pc-4** was observed at 10 and 50 μM, without the loss of cell viability (data not shown).

Light-induced toxicities of **ZnPc** and **Pc-4** in HSC-3 cells are shown in Table 6. The cells were incubated with **ZnPc** and **Pc-4** (0.1 and 5.0 μM) for 24 h, and subsequently exposed to light (650–850 nm) for 20 min with spectral irradiance at 89 and 36 mW/cm^2 at a distance of 5 and 10 cm from the light source, respectively. **Pc-4** was ineffective at 0.1 μM, while a low, approx. 15% photocytotoxicity was observed at 5 μM, at a distance of 5 and 10 cm. These values were significantly lower than the control cells. **ZnPc** at 0.1 μM decreased cell viability by 30% at a distance of 5 cm ($P < 0.005$), while 5 μM **ZnPc** caused 100% photocytotoxicity at a distance of 5 and 10 cm.

In conclusion, the photosensitizing effect of **Pc-4** was significantly lower than that of **ZnPc**. The efficacy of photosensitizer in photokilling of cultured cells is affected by its hydrophilic/hydrophobic properties. The cellular uptake of photosensitizer, which involves binding to the cell membrane receptor and subsequent internalization, is affected by hydrophobicity and the aggregation status of the photosensitizer. A very low phototoxicity of **Pc-4** originated most likely from the presence of eight ester-alkyloxy substituents (–O–$(CH_2)_3$–CO–OC_5H_{11}) in its molecule, which might lead to an increased hydrophobicity and tendency to aggregate. Attempts to encapsulate **Pc-4** in PG:PC and PG:CL multilamellar liposomes were unsuccessful (data not shown).

3. Conclusions

In conclusion, two novel zinc(II) phthalocyanines bearing non-peripheral ester-alkyloxy substituents (**Pc-4** and **Pc-5**) were synthesized, by a two-step procedure starting from 2,3-dicyanohydroquinone.

Both sensitizers show promising photophysical properties, including solvatochromic study, qualitative evaluation of emission, aggregation behavior and singlet oxygen generation. The emission spectra of **Pc-4** and **Pc-5**, similarly to the absorption ones, depend on the presence of heteroatoms in the macrocyclic periphery. Therefore a decrease of fluorescence quantum yield to the level of $\Phi_f = 0.06$ in comparison to that observed for **ZnPc** ($\Phi_f = 0.2$) was noticed. This process has been related to the presence of free electron pairs at the oxygen atoms substituted to the non-peripheral positions of **Pc-4** and **Pc-5**, which facilitates the nonradiative quenching being the result of their coupling with the π electron system of the phthalocyanine ring. It was proven that the photodynamic activity of the compounds studied depends on the molecular oxygen level, as bubbling with nitrogen *via* reaction vessel for 20 min led to distinct inhibition of the 1,3-diphenylisobenzofurane (DPBF) oxidation. Comparison of the quantum yields of singlet oxygen generation as well as the oxidation rate constants using DPBF before and after deaeration proved the photodynamic effect of **Pc-4** and **Pc-5** to be governed by the photosensitization mechanism II. Changes in the quantities of the compounds exposed to irradiation were also estimated. Upon their exposure to light the changes in intensity of the Q band were monitored. The photodecomposition of **Pc-4** and **Pc-5** in DMSO or DMF solutions was found to proceed according to the first order kinetic reaction in two stages.

The photosensitizing effect of **Pc-4** in HSC-3 cells was significantly lower than that of **ZnPc**. **Pc-4** was ineffective at 0.1 μM, while a low, approx. 15% photocytotoxicity was observed at 5 μM, at a distance of 5 and 10 cm. The efficacy of **Pc-4** in photokilling of cultured cells is affected by hydrophobicity and the aggregation status of the photosensitizer. Nevertheless, the behavior observed in homogeneous solution is not always the case in cellular systems, where the biological microenvironment of the phthalocyanines can induce significant changes in the photophysics of the sensitizers [15,40].

Further synthetic and physicalchemical studies concerning photosensitizers possessing reduced amount of ester-alkoxy substituents in the periphery of other groups of porphyrinoids are in progress in our laboratory.

4. Experimental

4.1. Synthesis

All reactions were conducted in oven dried glassware under argon. Reaction temperatures reported refer to external bath temperatures. All reagents were obtained from commercial suppliers and used without further purification. All solvents were rotary evaporated at or below 50 °C under reduced pressure. Melting points were obtained on a "Stuart" Bibby Sterlin Ltd® melting point apparatus and are uncorrected. Chromatography was carried out on Merck silica (eluants are given in parentheses). Dry flash column chromatography was carried out on silica gel 60, particle size 40–63 μm. Thin layer chromatography (TLC) was performed on silica gel 60 F_{254} plastic sheets and visualized with UV (λ_{max} 254 or 365 nm). Elemental analyses were determined by the Advanced Chemical Equipment and Instrumentation Facility at the Faculty of Chemistry, Adam Mickiewicz University in Poznan and the London Metropolitan Microanalytical Service. UV–Vis spectra were recorded on a Hitachi UV/VIS U-1900 and Shimadzu UV-160A. FT-IR measurements were collected on a Bruker Victor 22 and a Mattson 5000 spectrometers. ^{1}H and ^{13}C NMR spectra were recorded on a Bruker DRX-400 and 500 spectrometers. Chemical shifts (δ) are quoted in parts per million (ppm) and are referred to a residual solvent peak. Coupling constants (J) are quoted in Hertz (Hz) to the nearest 0.5 Hz. The abbreviations s, d, t, p, h, and m refer to singlet, doublet, triplet, pentet, hidden, and multiplet respectively. Additional techniques (^{1}H–^{1}H COSY (COrrelation SpectroscopY), ^{1}H–^{1}H TOCSY (TOtal Correlated SpectroscopY), HMQC (Heteronuclear Multiple Quantum Coherence), and HMBC (Heteronuclear Multiple Bond Correlation)) were used to assist allocation. Analyt-

ical HPLC was performed on a Agilent 1200 Series. Mass spectrometry (EI, ESI, MALDI TOF) were recorded by both the Imperial College London Department of Chemistry Mass Spectrometry and the Institute of Bioorganic Chemistry of the Polish Academy of Sciences in Poznan Services.

4.1.1. 3,6-Bis(ethyloxycarbonylmethyloxy)-1,2-benzenedicarbonitrile (**2**)

Ethyl bromoacetate (8.35 g, 50 mmol) was added to well-stirred slurry of 3,6-dihydroxy-1,2-benzenedicarbonitrile (3.20 g, 20 mmol) and anh. K_2CO_3 (5.53 g, 40 mmol) in DMF (50 mL), and heated at 70 °C for 24 h. The reaction contents were poured into water (400 mL), and the suspension was vigorously stirred. The resulting white solid was filtered under reduced pressure, washed with water, dried, heated under reflux in MeOH (70 mL) for 15 min to give white solid (**2**) (4.04 g, 60.8%). M.p. = 137–138 °C. R_f (CH_2Cl_2) 0.15. UV–Vis (MeOH): λ_{max} (log ε) = 223 (4.37), 333 (4.08). ^{1}H NMR (400 MHz, DMSO-d_6) δ = 7.57 (s, 2H, ArH), 5.06 (s, 4H, ArOCH_2), 4.17 (q, ^3J = 7.0 Hz, 4H, OCH_2), 1.21 (t, ^3J = 7.0 Hz, 6H, CH_3). ^{13}C NMR (100 MHz, DMSO-d_6) δ = 167.8 (C=O), 154.4 (Ar, C–O), 120.5 (Ar, C–H), 113.3 (CN), 103.2 (Ar, C–CN), 65.9 (ArOCH_2), 61.0 (OCH_2), 13.9 (CH_3). *Anal.* calcd for $C_{16}H_{16}N_2O_6{\cdot}0.5H_2O$: C, 56.30; H, 5.02; N, 8.21. Found: C, 56.14; H, 4.81; N, 8.20%.

4.1.2. 3,6-Bis[3-(ethyloxycarbonyl)propyloxy]-1,2-benzenedicarbonitrile (**3**)

Ethyl 4-bromobutyrate (9.75 g, 50 mmol) was added to a well-stirred slurry of 3,6-dihydroxy-1,2-benzenedicarbonitrile (3.20 g, 20 mmol) and anh. K_2CO_3 (5.53 g, 40 mmol) in DMF (50 mL), and heated at 70 °C for 24 h. The reaction contents were poured into water (400 mL), and the solution was vigorously stirred. The resulting white solid was filtered under reduced pressure, washed with water, dried, heated under reflux in MeOH (70 mL) for 15 min to give white solid (**3**) (7.16 g, 92.2%). M.p. = 140–141 °C. R_f (CH_2Cl_2) 0.22. UV–Vis (MeOH): λ_{max} (log ε) = 227 (4.31), 354.5 (3.59). ^{1}H NMR (400 MHz, DMSO-d_6) δ = 7.62 (s, 2H, ArH), 4.19 (t, ^3J = 6.5 Hz, 4H, ArOCH_2), 4.08 (q, ^3J = 7.0 Hz, 4H, OCH_2), 2.49 (t, ^3J = 7.0 Hz, 4H, CH_2CO), 2.00 (p, ^3J = 7.0 Hz, 4H, CH_2CH$_2$CO), 1.19 (t, ^3J = 7.0 Hz, 6H, CH_3). ^{13}C NMR (100 MHz, DMSO-d_6) δ = 172.8 (C=O), 155.2 (Ar, C–O), 121.0 (Ar, C–H), 113.9 (CN), 103.4 (Ar, C–CN), 69.3 (ArOCH_2), 60.4 (OCH_2CH$_3$), 30.2 (CH_2CH$_2$CO), 24.3 (CH_2CH$_2$CO), 14.5 (CH_3). HRMS (EI) calcd for $C_{20}H_{24}N_2O_6$ $[M]^+$ 388.1634, found 388.1637. MS (ESI) MH^+ 389, MK^+ 427. *Anal.* Calc. for $C_{20}H_{24}N_2O_6$: C, 61.84; H, 6.23; N, 7.21. Found: C, 61.70; H, 6.55; N, 7.23%.

4.1.3. 1,4,8,11,15,18,22,25-Octakis[(3-(pentyloxycarbonyl)propyloxy]-phthalocyaninato zinc(II) (***Pc-4***)

DBU (598 mg, 4 mmol) was added to the solution of **3** (1.55 g, 4 mmol) and $Zn(OAc)_2$ (367 mg, 2 mmol) in 1-pentanol (7 mL). The reaction mixture was stirred at 140 °C for 24 h. Next 1-pentanol was evaporated with toluene and dry residue was purified by silica gel chromatography (CH_2Cl_2:CH_3OH, 50:1 to 35:1) to give **Pc-4** (149 mg, 7.6%). R_f (CH_2Cl_2:CH_3OH, 10:1) 0.65. UV–Vis (CH_2Cl_2:CH_3OH): λ_{max} (log ε) = 328 (4.13), 489 (3.72), 768 (4.35), 810 (4.54). IR (cm^{-1}) 2927, 2856, 1732, 1498, 1383, 1265, 1192, 1054. ^{1}H NMR (400 MHz, pyridine-d_5) 7.87 (s, 8H), 5.16 (t, ^3J = 6.5 Hz, 16H), 4.09 (t, ^3J = 7.0 Hz, 16H), 3.08 (t, ^3J = 7.0 Hz, 16H), 2.69 (p, ^3J = 7.0 Hz, 16H), 1.48 (p, ^3J = 7.0 Hz, 16H), 1.16 (m, 32H), 0.74 (t, ^3J = 7.0 Hz, 24H). ^{13}C NMR (100 MHz, pyridine-d_5) 173.5, 153.0, 151.7, 128.3, 119.0, 71.4, 64.4, 30.9, 28.4, 28.0, 25.3, 22.3, 13.8 (Table 1S, Supplementary material). MS (MALDI) MH^+ 1953; HPLC: stationary phase – Eclipse XDB-C18, mobile phase – MeOH:THF:CH_2Cl_2 = 80:10:10 (v/v/v), UV detection at 735 nm, retention time 4.28 min, purity 96.81%.

4.1.4. 1,4,8,11,15,18,22,25-Octakis[3-(hexyloxycarbonyl) propyloxy]phthalocyaninato zinc(II) (***Pc-5***)

DBU (0.58 g, 3.9 mmol) was added to the solution of **3** (1.5 g, 3.9 mmol) and $Zn(OAc)_2$ (0.37 g, 2.0 mmol) in 1-hexanol (4 mL). The reaction mixture was stirred at 140 °C for 72 h. Next 1-hexanol was evaporated with toluene and dry residue was purified by silica gel chromatography (CH_2Cl_2:CH_3OH, 15:1 to 10:1) to give black green **Pc-5** (10 mg, 0.4%). R_f (CH_2Cl_2:MeOH, 10:1) 0.44. UV–Vis (MeOH): λ_{max} (log ε) = 238 (5.14), 367 (5.10), 662 (3.84), 736 (4.51). ^{1}H NMR (400 MHz, pyridine-d_5) 7.88 (s, 8H, ArH), 5.18 (t, ^3J = 7.0 Hz, 16H, ArOCH_2), 4.12 (t, ^3J = 7.0 Hz, 16H, OCH_2CH$_2$), 3.09 (t, ^3J = 7.0 Hz, 16H, CH_2CO), 2.71 (p, ^3J = 7.0 Hz, 16H, CH_2CH$_2$CO), 1.50 (p, ^3J = 7.0 Hz, 16H, OCH$_2$CH_2), 1.23–1.06 (bm, 48H, CH_2CH_2CH_2CH$_3$), 0.73 (t, ^3J = 7.0 Hz, 24H, CH_3). ^{13}C NMR (100 MHz, pyridine-d_5) 173.7, 153.2, 151.9, 128.6, 119.2, 71.6, 64.6, 31.6, 31.1, 28.9, 25.8, 25.6, 22.7, 14.1. MS (MALDI) MH^+ 2066; HPLC: stationary phase – Eclipse XDB-C18, mobile phase – MeOH:THF:CH_2Cl_2 = 80:10:10 (v/v/v); UV detection at 735 nm, retention time 8.61 min, purity 95.02%.

4.1.5. 1,4,8,11,15,18,22,25-Octakis[(3-(pentyloxycarbonyl) propyloxy]phthalocyanine (***Pc-6***)

DBU (0.25 g, 1.9 mmol) was added to the solution of **3** (0.75 g, 1.9 mmol) in 1-pentanol (6 mL). The reaction mixture was stirred at 135 °C for 24 h. Next 1-pentanol was evaporated with toluene and dry residue was purified by silica gel chromatography (CH_2Cl_2:CH_3OH, 50:1 to 10:1, next n-hexane:EtOAc, 7:1 to 1:1) to give green solid **Pc-6** (0.014 g, 1.6%). R_f (*n*-hexane:EtOAc, 7:4) 0.32. UV–Vis (CH_3OH): λ_{max} (log ε) = 233 (4.62), 323 (4.66), 740 (4.85). ^{1}H NMR (400 MHz, pyridine-d_5) 7.86 (s, 8H, ArH), 5.02 (th, 16H, ArOCH_2), 4.07 (t, ^3J = 7.0 Hz, 16H, OCH_2CH$_2$), 3.14 (t, ^3J = 7.0 Hz, 16H, CH_2CO), 2.69 (p, ^3J = 7.0 Hz, 16H, CH_2CH$_2$CO), 1.43 (p, ^3J = 7.0 Hz, 16H, OCH$_2$CH_2) 1.23–1.03 (bm, 32H, CH_2CH_2CH$_3$), 0.69 (t, ^3J = 7.0 Hz, 24H, CH_3), 0.18 (s, 2H, NH). MS (MALDI) MH^+ 1892.

4.1.6. 1,4,8,11,15,18,22,25-Octakis[3-(hexyloxycarbonyl) propyloxy]phthalocyanine (***Pc-7***)

DBU (304 mg, 2 mmol) was added to the solution of **3** (776 mg, 2 mmol) in 1-hexanol (2 mL). The reaction mixture was stirred at 140 °C for 24 h. Next 1-hexanol was evaporated with toluene and dry residue was purified by silica gel chromatography (CH_2Cl_2:CH_3OH, 25:1 to 10:1) to give **Pc-7** (47 mg, 4.7%). R_f (CH_2Cl_2:CH_3OH, 10:1) 0.86. UV–Vis (CH_2Cl_2:CH_3OH, 25:1): λ_{max} (log ε) = 328 (4.74), 401 (4.27), 762 (5.07), 852 (3.93); IR (cm^{-1}) 3301, 2955, 2930, 2858, 1732, 1599, 1503, 1383, 1269, 1175, 1059. ^{1}H NMR (500 MHz, pyridine-d_5) 7.87 (s, 8H, ArH), 5.07 (t, ^3J = 6.5 Hz, 16H), 4.09 (t, ^3J = 7.0 Hz, 16H), 3.15 (t, ^3J = 7.5 Hz, 16H), 2.70 (p, ^3J = 7.0 Hz, 16H), 1.44 (p, ^3J = 7.5 Hz, 16H), 1.13 (p, ^3J = 7.5 Hz, 16H), 1.06 (m, 32H), 0.71 (t, ^3J = 7.0 Hz, 24H), 0.19 (s, 2H). ^{13}C NMR (125 MHz, pyridine-d_5) 173.7, 152.0, 150.1^h, 127.0, 119.4, 71.4, 64.4, 31.5, 31.1, 28.9, 25.8, 22.7, 14.3 (Table 2S, Supplementary material). MS (MALDI) MH^+ 2005.

4.2. Photochemical and solvatochromic studies

All measurements were carried out on Shimadzu UV-160 A spectrophotometer with PC 160 Plus software. Solvents were obtained from commercial suppliers and used without further purification. UV–Vis spectra were recorded in the range of 300–900 nm. Molar extinction coefficients values were similar for both Pcs in DMSO and DMF (Table 7).

Table 7
Maximum absorptions and molar absorption coefficients of **Pc-4** and **Pc-5** in DMSO and DMF.

Solvent	Compound	λ_{max} (log ε)
DMSO	**Pc-4**	327 (4.60) 665 (4.51) 743 (5.20)
	Pc-5	327 (4.67) 665 (4.56) 743 (5.25)
DMF	**Pc-4**	326 (4.60) 660 (4.49) 736 (5.20)
	Pc-5	327 (4.61) 661 (4.52) 733 (5.20)

4.3. Emission properties

Fluorescence quantum yield measurements of the compounds under study were carried out in solutions in dimethylsulfoxide (DMSO for UV spectroscopy from *Fluka*, used as supplied). Absorbance of the solutions was kept below 0.1 at the maximum of the Q-band absorption in a 1-cm-thick cell in order to avoid the reabsorption of emitted photons. Zinc phthalocyanine (**ZnPc**, *Sigma–Aldrich*) was used as the standard ($\Phi_f = 0.20 \pm 0.03$) [37]. Stationary UV–Vis spectra were recorded using Cary Eclipse fluorescence and Cary 50 Scan absorption spectrophotometers from Varian.

4.4. Singlet oxygen generation

Solutions of diphenylisobenzofurane (DPBF) as singlet oxygen chemical quencher and photosensitizers in DMSO and DMF were irradiated in a 1 cm path length quartz cell with monochromatic light (sensitizer absorbance at Q band ~ 0.5) by a 150 W high-pressure Xe lamp (type XBO-150, *Optel*) through a monochromator (*Optel*). The light intensity was adjusted to 1.0 mW/cm^2 (Radiometer RD 0.2/2 with TD probe, *Optel*). Photooxidation reaction of DPBF was used to determine singlet molecular oxygen ($^1\Delta_g$) generation by the photosensitizers. The kinetics of DPBF photooxidation were studied by observing the decrease of the absorbance at $\lambda_{max} = 417$ nm. UV–Vis spectra were recorded on Shimadzu UV-160 A spectrophotometer with PC 160 Plus software. Zinc phthalocyanine (**ZnPc**, *Sigma–Aldrich*) was used as the standard. Measurements of the sample and reference under the same conditions enabled quantum yield calculation by direct comparison of the slopes in the linear region of the semilogarithmic plots of ln A_0/A vs. irradiation time obtained for the samples and corresponding slopes obtained for the reference. All the experiments were performed at ambient temperature. To avoid chain reactions induced by DPBF in the presence of singlet oxygen, the concentration of DPBF was set at $\sim 3 \times 10^{-5}$ mol L^{-1} and was kept the same for both the standard and the samples. Molar absorption coefficients (dm^3 mol^{-1} cm^{-1}) of DPBF at $\lambda = 417$ nm were determined as $\varepsilon = 19\,880$ in DMSO and $\varepsilon = 21\,821$ in DMF. Solutions of the sensitizer containing DPBF were prepared in the dark and irradiated in the Q band region. Additional experiments were also performed for each mixture of DPBF and photosensitizer after 20 min bubbling with nitrogen.

4.5. Photostability assay

Samples were illuminated under aerobic conditions according to the recommendations in the first version of the ICH Harmonised Tripartite Guideline – Q1B. The source of light was 150 W high-pressure Xe lamp (type XBO-150, *Optel*). The photodecomposition process for each compound was performed for Q band using a yellow glass cut-off filter HCC16 with maximal transmission between 600 and 800 nm. The intensity of radiation was measured by a luxometer (TES 1335, *TES Electrical Electronic Corp.*) and adjusted at 130 klux.

Prior to exposition solutions of **Pc-4**, **Pc-5** were transferred to a quartz cylindrical cell ($V = 2.7$ mL, $l = 1$ cm). The initial value of the absorbance at Q bands was between 0.7 and 0.8. The photostability of the compounds was evaluated in DMSO, DMF and THF. During exposure to light for certain periods of time, the UV–Vis spectra were recorded in the range of 200–800 nm.

Photodecomposition of phthalocyanines as a result of separate irradiation of Q bands was initially monitored qualitatively as explicit changes in the shape of the absorption spectra.

The process was also evaluated quantitatively. After certain time intervals of exposition, absorption values at characteristic wavelengths for each phthalocyanine were measured.

4.6. Biological activity

4.6.1. Chemicals

Zinc phthalocyanine (**ZnPc**, *Sigma–Aldrich*) and **Pc-4** were dissolved in DMSO (*Sigma–Aldrich*) to a final concentration of 9.8 mM. Dulbecco's modified Eagle's MEM medium with or without phenol red, penicillin–streptomycin solution, L-glutamine and trypsin–EDTA were obtained from the University of California San Francisco (UCSF) Cell Culture Facility (San Francisco, CA). Alamar Blue dye (alamarBlue™) was obtained from Biosource International, Inc. (Camarillo, CA). Lipids, L-α-phosphatidylcholine (Egg, Chicken) (PC), L-α-phosphatidylglycerol (Egg, Chicken) (sodium salt) (PG), and cardiolipin (1,3-bis(sn-3′-phosphatidyl)-sn-glycerol) (CL) (Heart, Bovine-Disodium Salt) were obtained from *Avanti Polar Lipids* (Birmingham, AL).

4.6.2. Cell culture

HSC-3 human squamous carcinoma cells, derived from the tongue [41], were provided by Dr. R. Kramer (UCSF). The cells were cultured in Dulbecco's modified Eagle's MEM supplemented with 10% (*v/v*) heat-inactivated fetal bovine serum (FBS), penicillin (100 U/mL), streptomycin (100 μg/mL) and L-glutamine (4 mM) (DMEM/10). The cells were incubated at 37 °C in a humidified atmosphere containing 5% CO_2 and were passaged 1:6 twice a week using trypsin–EDTA solution.

4.6.3. Dark toxicity

HSC-3 cells were seeded in 48-well plates at a density 1.8×10^5 cells per well in 1 ml of DME/10 1 day before the experiment, and used at approx. 80% confluence. Subsequently, cells were washed twice with phosphate buffer saline (PBS) and 1 mL of medium without FBS and phenol red, containing phosensitizer at a given concentration, was added to each well except controls. The FBS-free medium was used to avoid binding of the photosensitizers to serum proteins. After the 24 h incubation at 37 °C, cells were washed twice with PBS and cell viability was quantified by the Alamar Blue assay. Cells incubated either with DME medium alone or DME/0.5% DMSO served as controls.

4.6.4. Light-dependent toxicity

HSC-3 cells were seeded in 48-well plates at a density of 1.8×10^5 cells per well in 1 mL of DME/10 1 day before the experiment and used at approx. 80–90% confluence. Cells were prewashed twice with PBS, and 1 mL of medium without FBS and phenol red, containing 0.1 or 5 μM of a given phosensitizer, was added to each well except controls. Cells were incubated for 24 h at 37 °C, washed twice with PBS and then 0.5 mL of medium without FBS and phenol red was added. Subsequently, the cells were exposed to light (650–850 nm) from the light bulb (Dura Max 75 W Med 120 V A19 Cl/LL 20 W; *Philips Electronics North America Corporation*, *Andover*, *MA*), at a distance of 5 or 10 cm from the light bulb to the plate, for 20 min. The total spectral irradiance at the level of cells, and in the presence of a water filter, was 89 and 36 mW/cm^2 (650–

850 nm), measured using a radiometer RD 0.2/2 with TD probe (Optel). These measurements indicated that the irradiance was constant over the small area occupied by the 48-well plates. Infrared radiation was minimized using a 2 cm water filter between the cell plates and the light source. One plate from each experiment was not exposed to light and served as a control. Directly after light exposure, medium without FBS and phenol red was replaced with 1 mL of fresh DME/10, and cells were incubated for 24 h at 37 °C. Cell viability was quantified by the Alamar Blue assay.

4.6.5. Cell viability assay

Cell morphology was evaluated by inverted phase contrast microscopy at 25× magnification. The number of viable cells used for the experiments was determined by Trypan blue exclusion. Cell viability was quantified by a modified Alamar Blue assay [42,43]. Briefly, 1.0 mL of 10% (v/v) Alamar Blue dye in the DME/10 was added to each well. After incubation at 37 °C for 1.5–3 h, 200 μL of the supernatant was assayed by measuring the absorbance at 570 nm and 600 nm. Cell viability (as a percentage of control cells) was calculated according to the formula $[(A_{570} - A_{600})$ of test cells$] \times 100/[(A_{570} - A_{600})$ of control cells].

4.6.6. Statistical analysis

Data represent the mean ± standard deviation (SD) from two independent experiments performed in triplicate. Data were compared for statistical significance by the unpaired Student's *t*-test, using StatView software (BrainPower Inc., Calabasas, CA). A probability value (*P*) of less than 0.05 was considered significantly different.

Acknowledgments

This study was partially supported by grant from the Polish Ministry of Science and Higher Education (N405 031 32/2052). T.G. thanks Professor A.G.M. Barrett from the Imperial College in London and Professor S. Sobiak from the Poznan University of Medical Sciences for supporting his studies. P.F. thanks Professor E. Vauthey from the University of Geneva for supporting his studies and acknowledges the financial support from the Foundation for Polish Science. The authors thank Beata Kwiatkowska and Michael Yee for excellent technical assistance.

Appendix A. Supplementary data

Supplementary data associated with this article can be found, in the online version, at doi:10.1016/j.poly.2011.03.003.

References

[1] K.M. Smith, in: A.R. Katritzky, C.W. Rees (Eds.), Comprehensive Heterocyclic Chemistry, vol. 4, Pergamon, Oxford, 1984, pp. 377–442.
[2] M.P. Cormick, M. Rovera, E.N. Durantini, J. Photochem. Photobiol. A 194 (2008) 220.
[3] A. Diacon, L. Fara, C. Cincu, M.R. Mitroi, C. Zaharia, E. Rusen, C. Boscornea, C. Rosu, D. Comaneci, Opt. Mater. 32 (2010) 1583.
[4] Ş. Bayar, H.A. Dinçer, E. Gonca, Dyes Pigments 80 (2009) 156.
[5] T. Nyokong, Coord. Chem. Rev. 251 (2007) 1707.
[6] C.G. Claessens, W.J. Blau, M. Cook, M. Hanack, R.J.M. Nolte, T. Torres, D. Wöhrle, Monatsh. Chem. 132 (2001) 3.
[7] M. Kandaz, M.N. Yarasir, A. Koc, Polyhedron 28 (2009) 257.
[8] E.G.R. Fernandes, N.C.S. Vieira, A.A.A. de Queiroz, F.E.G. Guimaräes, V. Zucolotto, J. Phys. Chem. C 114 (2010) 6478.
[9] A.M. Saleh, A.O. Abu-Hilal, R.D. Gould, Curr. Appl. Phys. 3 (2003) 345.
[10] M.J. Cook, Pure Appl. Chem. 71 (1999) 2145.
[11] P. Juzenas, W. Chen, Y.P. Sun, M.A.N. Coelho, R. Generalov, N. Generalova, I.L. Christensen, Adv. Drug Deliver. Rev. 60 (2008) 1600.
[12] F. D'Souza, O. Ito, Coord. Chem. Rev. 249 (2005) 1410.
[13] M. Niemi, N.V. Tkachenko, A. Efimov, H. Lehtivuori, K. Ohkubo, S. Fukuzumi, H. Lemmetyinen, J. Phys. Chem. A 112 (2008) 6884.
[14] M.R. Ke, J.D. Huang, S.M. Weng, J. Photochem. Photobiol. A 201 (2009) 23.
[15] E.I. Yslas, V. Rivarola, E.N. Durantini, Bioorg. Med. Chem. 13 (2005) 39.
[16] I. Scalise, E.N. Durantini, Bioorg. Med. Chem. 13 (2005) 3037.
[17] J.P.F. Longo, S.P. Lozzi, A.R. Simioni, P.C. Morais, A.C. Tedesco, R.B. Azevedo, J. Photochem. Photobiol. B 94 (2009) 143.
[18] M.S. Ağırtaş, Dyes Pigments 79 (2008) 247.
[19] M. Durmuş, V. Ahsen, T. Nyokong, J. Photochem. Photobiol. A 186 (2007) 323.
[20] J.D. Spikes, J.E. van Lier, J.C. Bommer, J. Photochem. Photobiol. A 91 (1995) 193.
[21] K. Oda, S. Ogura, I. Okura, J. Photochem. Photobiol. B 59 (2000) 20.
[22] B. Akkurt, E. Hamuryudan, Dyes Pigments 79 (2008) 153.
[23] M. Durmuş, T. Nyokong, Polyhedron 26 (2007) 2767.
[24] J. Montanari, A.P. Perez, F. Di Salvo, V. Diz, R. Barnadas, L. Dicelio, F. Doctorovich, M.J. Morilla, E.L. Romero, Int. J. Pharm. 330 (2007) 183.
[25] F.L. Primo, M.M.A. Rodrigues, A.R. Simioni, M.V.L.B. Bentley, P.C. Morais, A.C. Tedesco, J. Magn. Magn. Mater. 320 (2008) e211.
[26] K. Zielińska, K.A. Wilk, E. Seweryn, J. Pietkiewicz, J. Saczko, Mater. Sci. Pol. 26 (2008) 443.
[27] I. Sircar, M. Hoefle, R.E. Maxwell, J. Med. Chem. 26 (1983) 1020.
[28] T.P. Forsyth, D. Bradley, G. Williams, A.G. Montalban, C.L. Stern, A.G.M. Barrett, B.M. Hoffman, J. Org. Chem. 63 (1998) 331.
[29] R.P. Linstead, M. Whalley, J. Chem. Soc. (1952) 4839.
[30] J. Vacus, G. Memetzidis, P. Doppelt, J. Simon, Chem. Commun. (1994) 697.
[31] M. Yousaf, M. Lazzouni, Dyes Pigments 28 (1995) 69.
[32] D.R. Lide (Ed.), CRC Handbook of Chemistry and Physics, vol. 78, CRC Press LLC, Boca Raton, 1997.
[33] A. Ogunsipe, M. Durmuş, D. Atilla, A.G. Gürek, V. Ahsen, T. Nyokong, Synthetic Met. 158 (2008) 839.
[34] W.F. Law, R.C. W Liu, J. Jiang, D.K. P Ng, Inorg. Chim. Acta 256 (1997) 147.
[35] A. Suchan, J. Nackiewicz, Z. Hnatejko, W. Wacławek, S. Lis, Dyes Pigments 80 (2009) 239.
[36] J.B. Birks, Photophysics of Aromatic Molecules, 1st ed., Wiley Monographs in Chemical Physics, Wiley-Interscience, London, 1970.
[37] A. Ogunsipe, D. Maree, T. Nyokong, J. Mol. Struct. 650 (2003) 131.
[38] W. Chidawanyika, E. Antunes, T. Nyokong, J. Photochem. Photobiol. A 195 (2008) 183.
[39] R. Bonnett, G. Martínez, Tetrahedron 57 (2001) 9513.
[40] B.M. Aveline, R.W. Redmond, Photochem. Photobiol. 69 (1999) 306.
[41] K. Matsumoto, M. Horikoshi, K. Rikimaru, S.A. Enomoto, J. Oral Pathol. Med. 18 (1989) 498.
[42] R.D. Fields, M.V. Lancaster, Am. Biotechnol. Lab. 11 (1993) 48.
[43] K. Konopka, E. Pretzer, P.L. Felgner, N. Düzgüneş, Biochim. Biophys. Acta 1312 (1996) 186.